

Sb-doped *p*-ZnO/Ga-doped *n*-ZnO homojunction ultraviolet light emitting diodes

S. Chu, J. H. Lim, L. J. Mandalapu, Z. Yang, L. Li, and J. L. Liu^{a)}

Quantum Structures Laboratory, Department of Electrical Engineering, University of California at Riverside, Riverside, California 92521, USA

(Received 25 January 2008; accepted 25 March 2008; published online 14 April 2008)

ZnO *p-n* homojunction light emitting diodes were fabricated based on *p*-type Sb-doped ZnO/*n*-type Ga-doped ZnO thin films. Low resistivity Au/NiO and Au/Ti contacts were formed on top of *p*-type and *n*-type ZnO layers, respectively. Au/NiO contacts on *p*-type ZnO exhibited a low specific resistivity of $7.4 \times 10^{-4} \Omega \text{ cm}^2$. The light emitting diodes yielded strong near-band-edge emissions in temperature-dependent and injection current-dependent electroluminescence measurements. © 2008 American Institute of Physics. [DOI: 10.1063/1.2908968]

ZnO recently has been extensively studied due to its wide band gap and large exciton binding energy for ultraviolet (UV)/blue optoelectronic applications such as light emitting diodes (LEDs) and laser diodes.^{1–4} Although it is extremely difficult to achieve reliable *p*-type ZnO due to compensation effect from shallow donors induced during material growth, many research groups have reported *p*-type ZnO and ZnO LEDs using various dopants such as N,^{5–7} P,^{8–10} As,^{11,12} and other specific techniques. Previously, Sb-doped *p*-type ZnO and *p-n* homojunction were studied by our group,^{13–15} however, no UV emissions were reported. In this letter, we report homojunction LEDs based on Sb-doped *p*-type ZnO that show strong near-band-edge (NBE) emissions at low temperatures and room temperature.

ZnO homojunction was grown on *n*-type Si (100) substrate (1–20 $\Omega \text{ cm}$) using molecular beam epitaxy system. First, a thin MgO buffer layer was deposited at 350 °C for 5 min to reduce the lattice mismatch between Si and ZnO,¹⁶ which was followed by the growth of a ZnO buffer layer at the same substrate temperature for 15 min. Then, the two layer structured Sb-doped *p*-type ZnO/Ga-doped *n*-type ZnO homojunction was grown on this MgO/ZnO buffer. The 420 nm thick Ga-doped ZnO film was deposited at a substrate temperature of 450 °C and Zn and Ga effusion cells temperatures of 380 and 520 °C, respectively. This was followed by the growth of the 420 nm thick Sb-doped ZnO layer under oxygen rich condition with a higher substrate temperature of 550 °C. During the growth of this layer, Zn and Sb effusion cell temperatures were 380 and 360 °C, respectively. *In situ* thermal activation of the Sb dopant was performed in vacuum at 750 °C for 20 min.

Homojunction LEDs were fabricated by standard photolithography techniques. Mesa size of $800 \times 800 \mu\text{m}^2$ were defined. Transmission line method (TLM) patterns with the size of $75 \times 50 \mu\text{m}^2$ and intercontact spacings of 10, 20, 30, and 40 μm were simultaneously made to study the contact properties. Etching was done using ammonium chloride hydroxide buffer solution to reach down to the *n*-type ZnO layer for *n*-type contacts with the etching rate of about 10 nm/min. Au/NiO and Au/Ti contacts of thicknesses of 500/30 and 150/30 nm were deposited on *p*-type Sb-doped

ZnO and *n*-type Ga-doped ZnO layer by e-beam evaporation, respectively. The contacts were subjected to rapid thermal annealing in nitrogen ambience to form Ohmic contacts. The annealing conditions of Au/NiO and Au/Ti contacts were 800 °C for 120 s and 400 °C for 60 s, respectively.

Current-voltage (*I-V*) characteristics were measured using Agilent 4155C semiconductor parameter analyzer. *I-V* curve in semilogarithmic scale of a typical device is shown in Fig. 1. The turn-on voltage of this diode is about 6 V, and the large turn-on voltage of the diode involves the effects from the voltage drop on the contact and *p*-type layer. The inset (a) of Fig. 1 gives the surface intercontact *I-V* curves of Au/NiO contacts on *p*-type ZnO and Au/Ti contacts on *n*-type ZnO, respectively, indicating Ohmic contact behavior. The electrical properties of the *n*-type ZnO layer were determined by Hall effect measurement in a van der Pauw configuration after the *p*-type ZnO layer was etched. Electron concentration, mobility, resistivity of $2.8 \times 10^{19} \text{ cm}^{-3}$, $8.7 \text{ cm}^2 \text{ V}^{-1} \text{ s}^{-1}$, and $0.02 \Omega \text{ cm}$, respectively, were obtained. For this multilayer structured device, electrical properties in *p*-type ZnO layer cannot be reliably obtained by Hall effect measurement. Nevertheless, *p*-type behavior of Sb-doped ZnO layer is evident from the rectifying diode characteris-

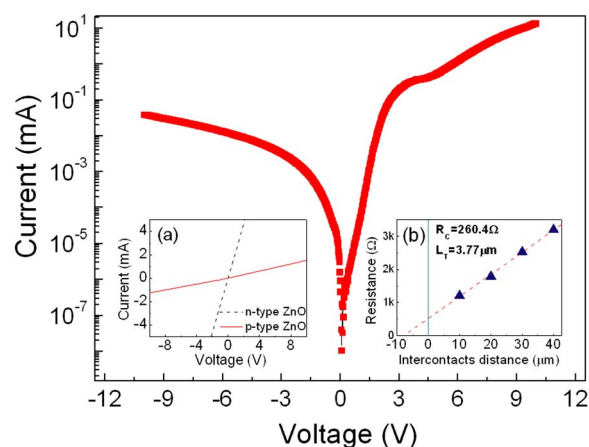


FIG. 1. (Color online) Semi-logarithmic scale *I-V* characteristics of the *p*-type Sb-doped ZnO/*n*-type Ga-doped ZnO homojunction. Inset (a) shows the surface *p-p* contacts and *n-n* contacts *I-V* curves, respectively. Ohmic contact behaviors are evident. Inset (b) gives the intercontact resistance as a function of intercontact distance for Au/NiO on *p*-type ZnO layers. Linear fitting was used to obtain the specific contact resistivity.

^{a)} Author to whom correspondence should be addressed. Electronic mail: jianlin@ee.ucr.edu.

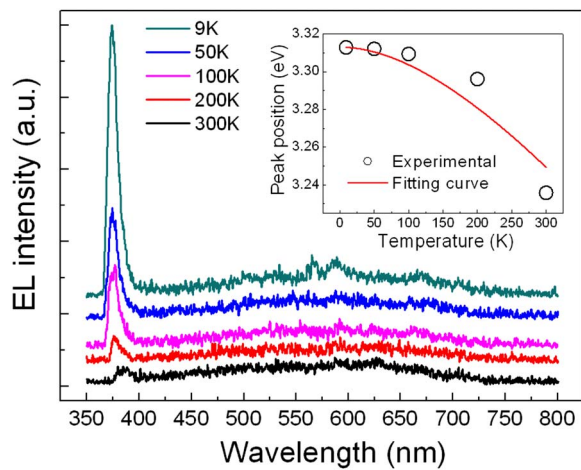


FIG. 2. (Color online) Temperature dependent EL spectra of homojunction diode from 9 to 300 K under injection current of 30 mA. The spectra are shifted on y scale for clarity. Inset shows the NBE peak positions as hollow circles against different temperatures and Varshni fitting is expressed as solid line.

tics. Low resistivity contacts are very important to ensure the high efficiency of ZnO optoelectronic device performance. Since we have relatively lightly doped *p*-type ZnO layer, Au/NiO contacts rather than Au/Ni contacts¹⁷ are chosen to form Ohmic contacts to the film in the devices. The total resistances (in TLM patterns) were plotted against the inter-contact distance in the inset (b) of Fig. 1. The contact resistance and transfer length are 260.4 Ω and 3.77 μm , which were extrapolated from linear fitting. Then the specific contact resistivity of $7.4 \times 10^{-4} \Omega \text{ cm}^2$ was calculated. This value is much smaller than that of the Au/Ni ($7.6 \times 10^{-3} \Omega \text{ cm}^2$) contacts on another piece of the same *p*-type ZnO layer. Furthermore, Au/Ni (500/30 nm) contacts need much higher annealing temperature to form reasonable Ohmic conduction (960 °C). Such a high temperature would potentially degrade the contact morphology and film quality. The advantage of Au/NiO contacts results from high *p*-type conductivity of NiO,¹⁸ and also the outdiffusion of oxygen could be reduced to depress oxygen vacancy in the film.¹⁷

Electroluminescence (EL) characterizations were performed by using home-built measurement setup including an Oriel monochromator and a lock-in amplifier with chopper. Temperature dependent EL spectra under 30 mA forward injection current are shown in Fig. 2. For the device operated at 9 K, the spectrum is dominated by a peak at 373.5 nm (3.32 eV). Schirra *et al.* recently assigned the ZnO 3.314 eV emission peak to the transition between free electron and a neutral acceptor level.¹⁹ However, considering the LT properties of our *p*-type film,¹³ we believe this peak is from band to band exciton recombination. The NBE peak shifts from 373.5 to 383.3 nm for temperature ranging from 9 to 300 K, which is shown in the inset of Fig. 2. The temperature dependence of the exciton energy in direct band-gap material follows Varshni equation, $E(T) = E(0) - \alpha T^2 / (T + \beta)$,²⁰ α and β are fitting parameters which are $\alpha = 0.00058 \text{ eV/K}$ and $\beta = 520 \text{ K}$. These values are close to reported results from Refs. 20 and 21 for ZnO materials. The peak values reasonably agree with the trend of the fitting curve, which indicates that the redshift of the peak is due to temperature induced band gap variation. In addition to the NBE peak, there seems to be broad radiative deep level emissions ranging from

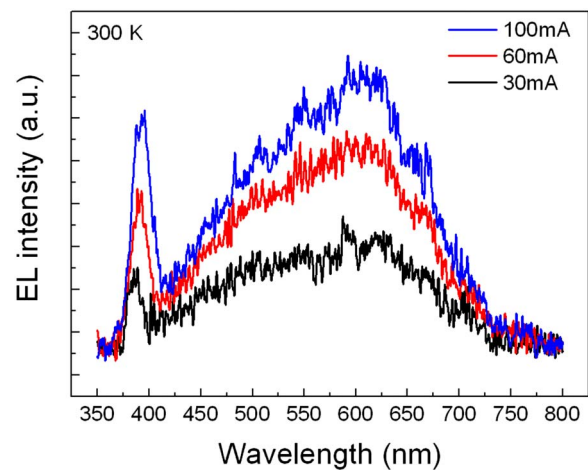


FIG. 3. (Color online) Room temperature EL spectra at different injection current from 30 to 100 mA.

400 to 800 nm. However, the magnitude drop of the deep level emission intensity is much less compared to NBE peak with increasing temperature. This may be attributed to more activation of nonradiative recombinations at higher temperatures, and also the bound exciton emissions quench at higher temperatures by thermal ionization of bound excitons.

Room temperature EL under different injection currents are shown in Fig. 3. For 30 mA injection current, the NBE peak is clearly seen at 383.3 nm (3.24 eV). The deep level emission at room temperature is mainly centered at 605 nm (2.05 eV), but with a shoulder around 490 nm (2.53 eV). The 490 nm band is commonly assigned to intrinsic defects.²² The 605 nm yellow band is attributed to oxygen interstitials,²³ which is consistent with the fact that the *p*-type ZnO was prepared in oxygen rich condition. The intensities of both NBE emission and emissions from deep levels increase with the increase of the injection current. The NBE emission redshifts from 383.3 nm (30 mA) to 390.9 nm (100 mA). This is also induced by the band gap variations, which result from the increased heating effects during the operation of LEDs. For example, the temperature of the diode is 490 K at the operation current of 100 mA from the inset of Fig. 2.

To further investigate the origin of these EL emissions, photoluminescence (PL) measurements were carried out on a separate piece of the sample annealed at 800 °C for 120 s, a process that was also used during the device fabrication. A 325 nm He–Cd laser was used as the excitation source. The room temperature PL spectra for both *p*-type layer and underneath *n*-type layer are shown in Fig. 4. PL of the *n*-type ZnO layer was obtained by etching away the *p*-type ZnO layer. Besides the NBE peak at 377.5 nm, emission bands centered around 520 nm are shown in both spectra and we consider that they are the same peak from *n*-type ZnO layer since it is commonly attributed to oxygen vacancy.²⁴ However, the *p*-type ZnO layer shows two more peaks at 480 and 610 nm which can closely link with the room temperature EL emissions of 490 and 605 nm. Thus, we believe that radiative recombinations in *p*-type layer, including NBE transitions, have contributed mainly to the observed EL spectra. Similar results were also observed in As-doped ZnO diode on GaAs substrate.¹² This is reasonable due to the fact that the concentration of holes in *p*-type ZnO layer is less than the electron concentration of *n*-type ZnO layer. As a result,

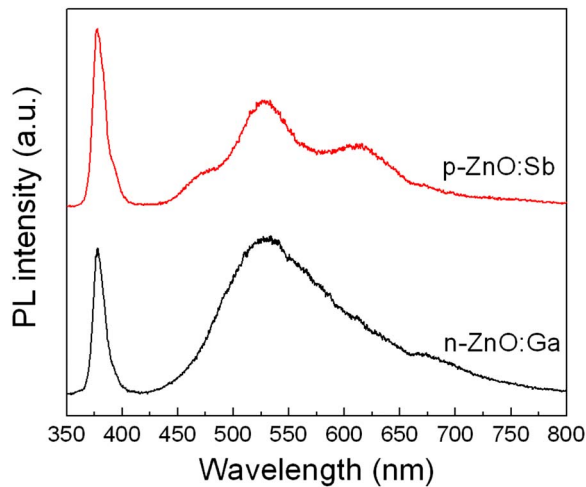


FIG. 4. (Color online) Room temperature PL spectra from Sb-doped *p*-type ZnO layer and Ga-doped *n*-type ZnO layer of the homojunction sample.

the depletion region mostly exists in the *p*-type layer, and the electron injection from the *n*-type layer to *p*-type layer dominates the recombination process.

In conclusion, ZnO homojunction LEDs with the Sb-doped *p*-type ZnO layer/Ga-doped *n*-type ZnO layer structure were fabricated and studied. The LEDs with the low resistivity Au/NiO contacts for *p*-type ZnO showed very good UV emissions at different temperatures and injection currents. This study suggests that Sb-doped *p*-type ZnO is promising for future ZnO optoelectronics.

This work was supported by the ONR/DMEA through the center for NanoScience and Innovation for Defense (CNID) under the Grant No. H94003-07-2-0703, and the UCEI grant.

¹Ü. Özgür, Ya. I. Alivov, C. Liu, A. Teke, M. A. Reshchikov, S. Dogan, V. Avrutin, S.-J. Cho, and H. Morkoç, *J. Appl. Phys.* **98**, 041301 (2005).
²S. J. Pearton, D. P. Norton, K. Ip, Y. W. Heo, and T. Steiner, *J. Vac. Sci.*

Technol. **B 22**, 932 (2004).

³D. C. Look, *Mater. Sci. Eng., B* **80**, 383 (2001).

⁴D. C. Look, B. Claflin, Y. I. Alivov, and S. J. Park, *Phys. Status Solidi A* **201**, 2203 (2004).

⁵A. Tsukazaki, A. Ohtomo, T. Onuma, M. Ohtani, T. Makino, M. Sumiya, K. Ohtani, S. F. Chichibu, S. Fuke, Y. Segawa, H. Ohno, H. Koinuma, and M. Kawasaki, *Nat. Mater.* **4**, 42 (2005).

⁶D. C. Look, D. C. Reynolds, C. W. Litton, R. L. Jones, D. B. Eason, and G. Cantwell, *Appl. Phys. Lett.* **81**, 1830 (2002).

⁷K. W. Liu, D. Z. Shen, C. X. Shan, J. Y. Zhang, B. Yao, D. X. Zhao, Y. M. Lu, and X. W. Fan, *Appl. Phys. Lett.* **91**, 201106 (2007).

⁸F. X. Xiu, Z. Yang, L. J. Mandalapu, J. L. Liu, and W. P. Beyermann, *Appl. Phys. Lett.* **88**, 052106 (2006).

⁹J. H. Lim, C. K. Kang, K. K. Kim, I. K. Park, D. K. Hwang, and S. J. Park, *Adv. Mater. (Weinheim, Ger.)* **18**, 2720 (2006).

¹⁰D. K. Hwang, M. S. Oh, J. H. Lim, C. G. Kang, and S. J. Park, *Appl. Phys. Lett.* **90**, 021106 (2007).

¹¹Y. R. Ryu, T. S. Lee, J. A. Lubguban, H. W. White, B. J. Kim, Y. S. Park, and C. J. Youn, *Appl. Phys. Lett.* **88**, 241108 (2006).

¹²J. C. Sun, J. Z. Zhao, H. W. Liang, J. M. Bian, L. Z. Hu, H. Q. Zhang, X. P. Liang, W. F. Liu, and G. T. Du, *Appl. Phys. Lett.* **90**, 121128 (2007).

¹³F. X. Xiu, Z. Yang, L. J. Mandalapu, D. T. Zhao, and J. L. Liu, *Appl. Phys. Lett.* **87**, 252102 (2005).

¹⁴L. J. Mandalapu, F. X. Xiu, Z. Yang, and J. L. Liu, *Appl. Phys. Lett.* **88**, 112108 (2006).

¹⁵L. J. Mandalapu, Z. Yang, F. X. Xiu, and J. L. Liu, *Appl. Phys. Lett.* **88**, 092103 (2006).

¹⁶M. Fujita, M. Sasajima, Y. Deesirapipat, and Y. Horikoshi, *J. Cryst. Growth* **278**, 293 (2005).

¹⁷L. J. Mandalapu, Z. Yang, and J. L. Liu, *Appl. Phys. Lett.* **90**, 252103 (2007).

¹⁸H. Ohta, M. Hirano, K. Nakahara, H. Maruta, T. Tanabe, M. Kamiya, T. Kamiya, and H. Hosono, *Appl. Phys. Lett.* **83**, 1029 (2003).

¹⁹M. Schirra, R. Schneider, A. Reiser, G. M. Prinz, M. Feneberg, J. Biskupek, U. Kaiser, C. E. Krill, R. Sauer, and K. Thonke, *Physica B* **401**, 362 (2007).

²⁰T. Shimomura, D. Kim, and M. Nakayama, *J. Lumin.* **112**, 191 (2005).

²¹S. J. Chen, Y. C. Liu, J. Y. Zhang, Y. M. Lu, D. Z. Shen, and X. W. Fan, *J. Phys.: Condens. Matter* **15**, 1975 (2003).

²²A. Ortiz, C. Falcony, J. Hernandez, M. Garcia, and J. C. Alonso, *Thin Solid Films* **293**, 103 (1997).

²³X. L. Wu, G. G. Siu, C. L. Fu, and H. C. Ong, *Appl. Phys. Lett.* **78**, 2285 (2001).

²⁴F. K. Shan, G. X. Liu, W. J. Lee, and B. C. Shin, *J. Appl. Phys.* **101**, 053106 (2007).